

ChemComm

Accepted Manuscript



This is an *Accepted Manuscript*, which has been through the Royal Society of Chemistry peer review process and has been accepted for publication.

Accepted Manuscripts are published online shortly after acceptance, before technical editing, formatting and proof reading. Using this free service, authors can make their results available to the community, in citable form, before we publish the edited article. We will replace this *Accepted Manuscript* with the edited and formatted *Advance Article* as soon as it is available.

You can find more information about *Accepted Manuscripts* in the [Information for Authors](#).

Please note that technical editing may introduce minor changes to the text and/or graphics, which may alter content. The journal's standard [Terms & Conditions](#) and the [Ethical guidelines](#) still apply. In no event shall the Royal Society of Chemistry be held responsible for any errors or omissions in this *Accepted Manuscript* or any consequences arising from the use of any information it contains.



Journal Name

COMMUNICATION

PLA₂-responsive and SPIO-loaded phospholipid micelles

Qiang Gao,^{a,b} Lesan Yan,^a Michael Chiorazzo,^c E. James Delikatny,^c Andrew Tsourkas^a and Zhiliang Cheng^{*a}

Received 00th January 20xx,
Accepted 00th January 20xx

DOI: 10.1039/x0xx00000x

www.rsc.org/

A PLA₂-responsive and superparamagnetic iron oxide (SPIO) nanoparticle-loaded phospholipid micelle was developed. The release of phospholipid-conjugated dye from these micelles was triggered due to phospholipid degradation by phospholipase A₂. High relaxivity of the encapsulated SPIO could enable non-invasive magnetic resonance imaging.

Phospholipase A₂ (PLA₂) specifically recognizes and catalytically hydrolyzes phospholipids at the sn-2 position to form fatty acid and lysophospholipid products. Elevated levels of PLA₂ have been associated with a number of diseases and pathologies including atherosclerosis,¹ pancreatitis,² acute sepsis,³ and cancer.⁴ For example, in prostate cancer PLA₂ levels have been found to be up to 22-fold higher than physiological levels.⁵⁻⁷ Thus it has been suggested that PLA₂ enzymes can serve as a novel diagnostic and therapeutic target for certain diseases.

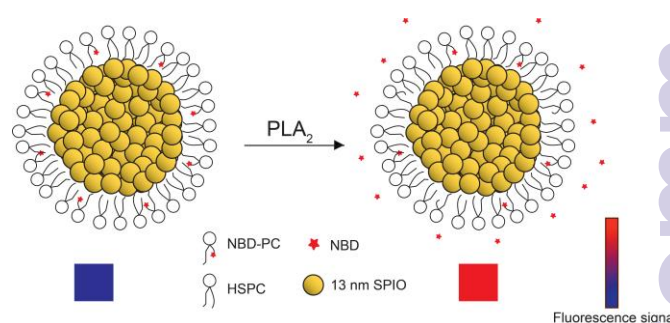
To date, a substantial amount of effort has been made in developing novel drug delivery system that seeks to concentrate the therapeutic agents in the desired sites while reducing the relative concentration in healthy tissues. One promising approach involves the use of stimulus-responsive nanoparticles that require endogenous or external stimuli to trigger drug release. The ability to limit drug release to a particular location can lead to lower off-target toxicity and improve the therapeutic index.⁸ While many types of stimuli including pH, temperature, light, ultrasound and proteolysis have been explored,⁹⁻¹¹ few studies have utilized PLA₂ to trigger drug release.¹²

Successful nanoparticle-based drug delivery is a very complicated process that involves the distribution, metabolism and excretion of the drug. The ability to non-invasively track nanoparticles following their administration is therefore expected to be highly valuable. A promising strategy for achieving this goal is to develop multifunctional nanoparticles that combine therapeutic

and diagnostic functions within a single nanoformulation, i.e. “theranostic” agents.¹³ It is expected that theranostic agents could provide important insight into localization of the drug and allow pathological processes to be monitored longitudinally.

Currently, a wide range of nanoparticle platforms including dendrimers,¹⁴ liposomes,¹⁵ polymersomes,¹⁶ micelles,¹⁷ emulsions,¹⁸ and silica nanoparticles,¹⁹ have been tested as platforms for drug nanocarriers. Among the many nanoparticle systems, phospholipid-based micelles are particularly attractive due to the recognized and tested biocompatibility of many phospholipids as well as their controlled size, ability to solubilize hydrophobic drugs/imaging agents, and favorable pharmacokinetics.^{20,21}

Herein, we report the design and testing of a PLA₂-responsive and superparamagnetic iron oxide (SPIO) nanoparticle-loaded phospholipid micelle (Scheme 1). It was expected that PLA₂-responsive phospholipid micelles loaded with SPIO nanoparticles could provide drug release specifically in response to PLA₂ activity and also enable non-invasive magnetic resonance (MR) imaging.



Scheme 1 Schematic diagram of PLA₂-responsive and SPIO-loaded phospholipid micelle.

Oleic acid-stabilized hydrophobic SPIONs were synthesized with mean diameters of approximately 13 nm. Transmission electron microscopy (TEM) images revealed a narrow distribution of spherical SPIOs (Supp. Figure S1A). Using an oil-in-water emulsion method,²² the small hydrophobic SPIONs were encapsulated within the hydrophobic core of micelles formed with the phospholipids.

^a Department of Bioengineering, University of Pennsylvania, Philadelphia, Pennsylvania 19104, United States. Email: zchen@seas.upenn.edu; Fax: 215-573-2071; Tel: 215-898-6030

^b Key Laboratory of Applied Surface and Colloid Chemistry, Ministry of Education, School of Chemistry and Chemical Engineering, Shaanxi Normal University, Xi'an, 710062, China

^c Department of Radiology, School of Medicine, University of Pennsylvania, Philadelphia, Pennsylvania 19104, United States

† Electronic Supplementary Information (ESI) available: [detailed experimental procedure]. See DOI: 10.1039/x0xx00000x

hydrogenated soy phosphatidylcholine (HSPC) and the fluorescent lipid 1-palmitoyl-2-[(7-nitro-2-1,3-benzoxadiazol-4-yl)amino]hexanoyl}-sn-glycero-3-phosphocholine (NBD-PC). The fluorophore NBD was attached to the sn-2 position of the phospholipid with a spacer (C6) between NBD and the lipid backbone, which was used to mimic a PLA₂-responsive prodrug. It was hypothesized that PLA₂ could specifically recognize and catalytically hydrolyze the sn-2 acyl bond of NBD-PC, resulting in the release of NBD. SPIO-loaded phospholipid micelles possessed a mean hydrodynamic diameter of 100 nm and low polydispersity (PDI <0.25) as determined by dynamic light scattering (DLS; Figure 1A). Due to the amphipathic properties of phospholipid molecules, these SPIO-micelles were highly soluble in aqueous solutions. TEM further confirmed the encapsulation of the SPIO within the micelles (Supp. Figure S1B). The SPIO-micelles observed by TEM were approximately spherical in shape with tightly packed clusters of SPIO encapsulated within the hydrophobic core. To assess the paramagnetic properties of the SPIO-loaded phospholipid micelles, the amount of iron (Fe) within the sample was determined by inductively coupled plasma optical emission spectroscopy (ICP-OES). The transverse r₂ relaxivity was then calculated as the slope of the curves 1/T₂ vs. Fe concentration, as shown in Figure 1B. T₂ (transverse relaxation times) were determined using a Bruker mq60 MR relaxometer operating at 1.41 T (60 MHz) and at 40 °C. It was found that SPIO-loaded micelles had an r₂ of 90 mM⁻¹s⁻¹. It should be noted that since tens of hydrophobic SPIO nanoparticles can be encapsulated within each 100 nm micelle, the SPIO-loaded micelles can generate a relaxivity that is amplified by a factor of 10 or more on a per particle basis, compared to a single SPIO nanoparticle. Therefore, it is expected that these agents are sufficiently sensitive for noninvasive MR imaging and tracking.

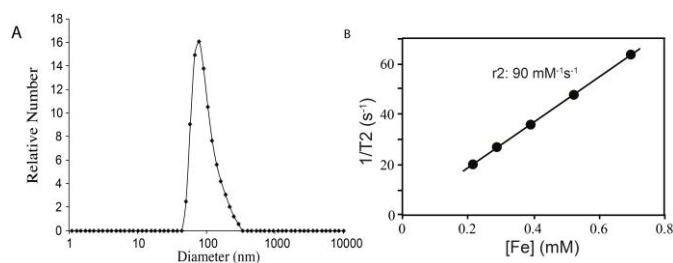


Figure 1. Characterization of SPIO-loaded phospholipid micelles. (A) Number-weighted size distribution of SPIO-loaded phospholipid micelles. (B) Relaxivity determination for SPIO-loaded phospholipid micelles.

As seen in Figure 2A, dissolution of the SPIO-micelles with surfactant Triton X-100 led to a significant increase in fluorescence. These findings imply that the NBD is highly quenched within the SPIO-micelle. There are two factors that likely contribute to the highly quenched state of NBD, self-quenching due to the high loading density (i.e. 10mol%) of NBD-PC within the micelles and quenching through interactions with the encapsulated SPIO nanoparticles. To explore the impact of self-quenching alone on NBP fluorescence, phospholipid micelles doped with 10mol% NBP-PC were prepared in the absence of SPIO nanoparticles and fluorescence was recorded before and after the addition of Triton X-100. It was found that in the absence of SPIO nanoparticles,

fluorophore-fluorophore interactions alone led to more than 90% quenching of NBP fluorescence. Therefore, it is likely that this was the primary mechanism responsible for a low NBP signal in the micelles (Supp. Figure S2). The presence of SPIO nanoparticles further reduced fluorescence of the micelles. As a result, dissolution of the SPIO-micelles led to a ~30-fold increase in NBP fluorescence compared with ~15-fold for the empty micelles (Figure 2B). Because of the efficient quenching of NBP fluorescence in the SPIO-micelles, it was expected that the PLA₂-triggered release of NBD could be monitored fluorometrically.

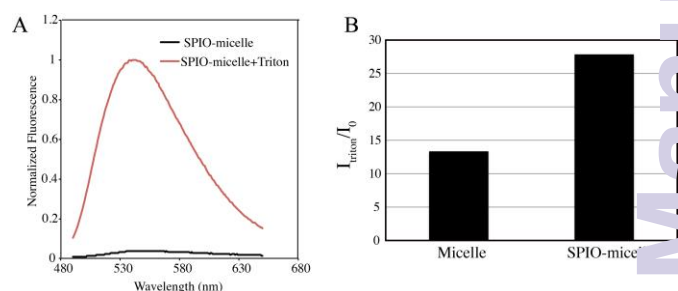


Figure 2. (A) Fluorescence quenching of NBD-PC in SPIO-loaded phospholipid micelles. The normalized fluorescence quenching was determined by subsequently lysing the micelles with Triton-X and measuring the total unquenched fluorescence intensity of the NBP-PC. (B) Quantitative analysis of fluorescence enhancement of NBP-PC in micelles or SPIO-loaded micelles, following lysis with Triton-X.

When SPIO-loaded micelles were incubated in 10 mM HEPES buffer, little to no change in fluorescence was observed over a 24 h time period. However, a significant increase in fluorescence intensity was observed immediately upon the addition of PLA₂ (Figure 3A). It should be noted that secreted PLA₂ was used in this study. The PLA₂-induced change in fluorescence was presumably due to the release of NBD into the surrounding bulk solution upon the hydrolysis of the phospholipid membrane by PLA₂. The released NBD led to fluorescence dequenching, resulting in a higher fluorescence intensity compared with fluorescence intensity from the SPIO-loaded-micelles. Furthermore, this change was time and concentration dependent. The intensity of fluorescence increased with increasing PLA₂ concentration in the range of 0 to 300 unit/mL. In addition, the rate of increase in fluorescence increased with PLA₂ concentration.

To further confirm that the measured changes in fluorescence signal were specifically caused by PLA₂-mediated mechanisms, experiments were also performed under two different conditions. First, SPIO-loaded micelles were incubated with PLA₂ in the media containing the calcium chelator EGTA (ethylene glycol tetraacetic acid). As expected, no change in fluorescence was observed since the activity of this PLA₂ enzyme is calcium-dependent (Figure 3B,^{23, 24}). Second, studies were performed by incubating the SPIO-micelles with both PLA₂ and increasing concentrations of the enzyme inhibitor LY311727. Under these conditions, LY311727 inhibited PLA₂ activity and led to a reduction in the extent of fluorescence activation in a concentration dependent manner (Figure 3C). These results confirm that the observed changes in fluorescence were PLA₂-specific.

In this work we developed PLA₂-responsive SPIO-loaded phospholipid micelles. The release of phospholipid-conjugated dye from these micelles was triggered due to phospholipid hydrolysis by PLA₂. Furthermore, many small hydrophobic SPIO nanoparticles were encapsulated within the micelle core, which could serve as highly efficient MR contrast agent for in vivo imaging. As a consequence, future work will be aimed at developing PLA₂-responsive multifunctional micelles containing therapeutic (i.e. phospholipid-conjugated prodrug), imaging (i.e. SPIO), and targeting agents.

μM. For all studies, the final concentration (Fe) of SPIO-loaded micelles and Ca²⁺ in the HEPES buffer (10 mM, pH 7.4) was 16 μg/mL and 2 mM, respectively. For B&C, the final concentration of PLA₂ in the buffer was 60 U/L. The black arrow indicated the time for the adding PLA₂. All experiments were performed at room temperature.

This work was supported in part by the National Institutes of Health (NIH) NCI R01CA157766 (AT) and NCI R01CA175480 (ZC). Q. G. thanks the China Scholarship Council and the National Nature Science Foundation of China (Nos. 21175089) for financial support.

References

- K. Kugiyama, Y. Ota, K. Takazoe, Y. Moriyama, H. Kawano, Y. Miyao, T. Sakamoto, H. Soejima, H. Ogawa, H. Doi, S. Sugiyama and H. Yasue, *Circulation*, 1999, **100**, 1280-1284.
- N. Agarwal and C. S. Pitchumoni, *Am J Gastroenterol*, 1991, **86**, 1385-1391.
- J. A. Green, G. M. Smith, R. Buchta, R. Lee, K. Y. Ho, I. A. Rajkovic and K. F. Scott, *Inflammation*, 1991, **15**, 355-367.
- T. Abe, K. Sakamoto, H. Kamohara, Y. Hirano, N. Kuwahara and M. Ogawa, *Int J Cancer*, 1997, **74**, 245-250.
- M. I. Patel, J. Singh, M. Niknami, C. Kurek, M. Yao, S. Lu, F. Maclean, N. J. C. King, M. H. Gelb, K. F. Scott, P. J. Russell, J. Boulas and Q. Dong, *Clin Cancer Res*, 2008, **14**, 8070-8079.
- J. Z. Jiang, B. L. Neubauer, J. R. Graff, M. Chedid, J. E. Thomas, N. W. Roehm, S. B. Zhang, G. J. Eckert, M. O. Koch, J. N. Eble and L. Cheng, *Am J Pathol*, 2002, **160**, 667-671.
- P. Sved, K. F. Scott, D. McLeod, N. J. C. King, J. Singh, M. Tsatralis, B. Nikolov, J. Boulas, L. Nallan, M. H. Gelb, M. Sajinovic, G. G. Graham, P. J. Russell and Q. H. Dong, *Cancer Res*, 2004, **64**, 6934-6940.
- S. R. MacEwan, D. J. Callahan and A. Chilkoti, *Nanomedicine (Lond)*, 2010, **5**, 793-806.
- M. Motornov, Y. Roiter, I. Tokarev and S. Minko, *Prog Polym Sci*, 2010, **35**, 174-211.
- S. Ganta, H. Devalapally, A. Shahiwala and M. Amiji, *J Control Release*, 2008, **126**, 187-204.
- S. Mura, J. Nicolas and P. Couvreur, *Nat Mater*, 2013, **12**, 991-1003.
- A. Dahan, R. Duvdevani, I. Shapiro, A. Elmann, E. Finkelstein and A. Hoffman, *J Control Release*, 2008, **126**, 1-9.
- Z. L. Cheng, A. Al Zaki, J. Z. Hui, V. R. Muzykantov and A. Tsourkas, *Science*, 2012, **338**, 903-910.
- Y. E. Kurtoglu, R. S. Navath, B. Wang, S. Kannan, R. Romero and R. M. Kannan, *Biomaterials*, 2009, **30**, 2112-2121.
- Z. L. Cheng, A. K. Chen, H. Y. Lee and A. Tsourkas, *Small*, 2010, **6**, 1398-1401.
- M. S. Kim and D. S. Lee, *Chem Commun*, 2010, **46**, 4481-4483.
- C. Y. Zhan, B. Li, L. J. Hu, X. L. Wei, L. Y. Feng, W. Fu and V. Y. Lu, *Angew Chem Int Edit*, 2011, **50**, 5482-5485.
- J. J. Wang, K. C. Sung, O. Y. P. Hu, C. H. Yeh and J. Y. Fang, *Control Release*, 2006, **115**, 140-149.
- I. I. Slowing, J. L. Vivero-Escoto, C. W. Wu and V. S. Y. Li, *Adv Drug Deliver Rev*, 2008, **60**, 1278-1288.
- R. R. Sawant and V. P. Torchilin, *Mol Membr Biol*, 2010, **27**, 232-246.
- A. N. Lukyanov and V. P. Torchilin, *Adv Drug Deliver Rev*, 2004, **56**, 1273-1289.
- A. Al Zaki, D. Joh, Z. L. Cheng, A. L. B. De Barros, G. K. Dorsey and A. Tsourkas, *ACS Nano*, 2014, **8**, 104-112.
- R. Raghupathi and R. C. Franson, *Biochim Biophys Acta*, 1992, **1126**, 206-214.
- Z. L. Cheng and A. Tsourkas, *Sci Rep-Uk*, 2014, **4**, 6958.

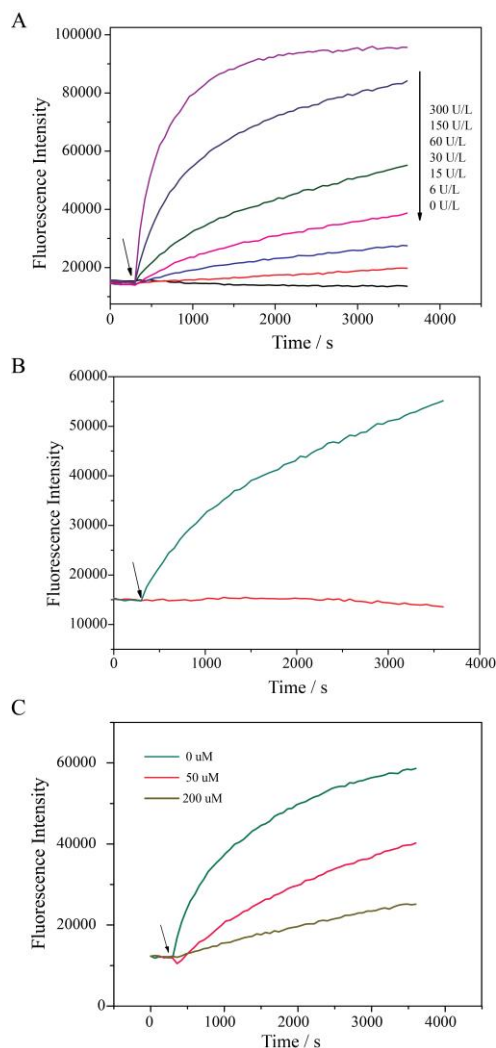


Figure 3. PLA₂ responsive SPIO-loaded phospholipid micelles. (A) SPIO-loaded phospholipid micelles were incubated with PLA₂ from 0 to 300 U/L. (B) PLA₂ was added to SPIO-loaded phospholipid micelles in the absence (blue curve) and presence of excess EGTA (red curve). (C) PLA₂ was added to SPIO-loaded phospholipid micelles in the presence of PLA₂ inhibitor LY 311727 from 0 to 200